

Cardiac output and peripheral resistance during larval development in the anuran amphibian *Xenopus laevis*

PING-CHUN LUCY HOU AND WARREN W. BURGGREN

Department of Biology, National Cheng Kung University, Tainan, Taiwan, Republic of China; and Department of Biological Sciences, University of Nevada, Las Vegas, Nevada 89154

Hou, Ping-Chun Lucy, and Warren W. Burggren.

Cardiac output and peripheral resistance during larval development in the anuran amphibian *Xenopus laevis*. *Am. J. Physiol.* 269 (*Regulatory Integrative Comp. Physiol.* 38): R1126–R1132, 1995.—Stroke volume (SV) and cardiac output (CO) were measured in anesthetized larvae of *Xenopus laevis* from hatching (3 mg) to the end of metamorphosis (~1 g). CO and SV were calculated from videotaped images of the intact beating heart. SV increased from 2.4×10^{-3} μl at 3 mg body mass to 7.6 μl at 1 g. CO increased from 0.25 $\mu\text{l}/\text{min}$ at 3 mg to 623 $\mu\text{l}/\text{min}$ at 1 g. With use of CO, along with arterial pressures from another study [P.-C. L. Hou and W. W. Burggren. *Am. J. Physiol.* 269 (*Regulatory Integrative Comp. Physiol.* 38): R1120–R1125, 1995], peripheral resistance and cardiac work were also calculated. Resistance decreased rapidly from 701 peripheral resistance units (PRU, $\text{mmHg} \cdot \text{s} \cdot \text{mm}^{-3}$) at 3 mg body mass to 79 PRU at 20 mg and gradually declined toward 0.9 PRU at 1 g. Cardiac work increased from 0.06 $\text{dyn} \cdot \text{mm}$ at 3 mg body mass to 1.27 $\text{dyn} \cdot \text{mm}$ at 20 mg and then climbed sharply to 717 $\text{dyn} \cdot \text{mm}$ at 1 g. The general pattern of change in hemodynamic variables (except heart rate) during larval development is similar in *Xenopus laevis* and chick embryos, suggesting a common pattern for hemodynamic development in vertebrate embryos/larvae.

cardiovascular function; stroke volume; cardiac work; ontogeny; amphibians

current major paradigm for vertebrate hemodynamic development. Such comparisons are essential in determining whether there is a common vertebrate pattern of cardiovascular physiological development in early embryonic stages.

In another study (15), we measured heart rate and blood pressure in developing *Xenopus laevis*. We tested the hypotheses that heart rate would scale allometrically with body mass and that blood pressure would increase in proportion to body mass. We found that heart rate declined in larval *Xenopus* during development at a much slower rate than would be predicted from allometric equations based on interspecific comparisons in adult vertebrates. Arterial blood pressure increased continuously from larvae to the adult.

The present study presents measurements of stroke volume, cardiac output, and peripheral resistance as a function of development in *X. laevis*. We test the hypothesis that total cardiac output increases during development in proportion to growth of new body mass and that the addition of new vessels will be reflected in reduced peripheral resistance, as described for the chick embryo.

MATERIALS AND METHODS

Animals

Larval *X. laevis* were obtained and reared as described earlier (15). Forty-three animals from stage 41 (newly hatched) of the Nieuwkoop-Faber (NF) larval staging system (21) to NF stage 66 (newly metamorphosed) were studied. Body mass ranged from 3 mg to 1.026 g.

Experimental Protocol for Stroke Volume Measurement

Larvae were anesthetized and prepared as described previously for heart rate and blood pressure measurement (15). Measurements were performed 30–180 min after anesthesia, as described below. Anesthetic bath temperature for all animals was 20–24°C, but the temperature range for any individual animal was only 1–2°C. At end of the measurements, the animal was killed and weighed. For small larvae (< stage 47), the pooled mass of two to five animals was measured, and mean body mass then used as individual mass for each animal.

Stroke Volume Measurement

Video and analytic equipment. Stroke volume was determined as the difference between end-diastolic (EDV) and end-systolic volume (ESV) of the ventricle. EDV and ESV were calculated from video images of the ventricle, as described below. Complete cardiac cycles of the ventricle were recorded with a Panasonic model WV-1550 black-and-white TV camera attached to a Wild M5 dissecting microscope, which was used to view the intact beating heart. The video camera, operating at 30 frames/s, was connected to a Panasonic Omnivision II video recorder. Continuous cardiac cycles were recorded on VHS tapes.

SURPRISINGLY LITTLE is known of the early development of cardiovascular function in vertebrates. The relatively few studies have focused on the chick embryo, with data available on cardiac output, central blood pressures, and peripheral resistance (1, 7–12, 14, 18). Heart rate in the chick embryo is variously reported to increase progressively, peak midway, or remain constant through incubation (9, 16, 18, 31), whereas cardiac output and blood pressure increase (10, 12, 18). Peripheral resistance decreases dramatically and cardiac work increases exponentially in the developing chick embryos (18).

Recently, studies of the functional development of the cardiovascular system have been expanded to anuran amphibian larvae (2–6, 17, 22, 24, 25). These studies in amphibians have focused primarily on heart rate (which decreases during development), blood pressure (which increases during development), and the pharmacological properties of cardiac muscle (which change in complex ways during development). Few studies have reported cardiac output (17, 22), and no single investigation of amphibian larvae has determined pressure and flow relationships from which important variables such as cardiac work and peripheral resistance could be calculated. Consequently, hemodynamic development in anuran amphibian larvae has not been compared in any systematic fashion with that in chick embryos, the

The video-recorded cardiac cycles were subsequently analyzed with a personal computer equipped with a video hardware card (PCVISIONplus Video Card, Imaging Technology, Woburn, MA) and an image analysis program (MeasurementTV, Garr Updegraff and DataCrunch, San Clemente, CA). Frames containing the ventricle at exactly end systole and end diastole, as judged by ventricle size, were selected for measurement of EDV and ESV (see selection protocol described below). Length-width measurements of the ventricle were obtained on the basis of epicardial outlines. Size calibration of the video image was performed by videotaping a 0.3125-mm-diameter metal rod with use of the same magnification used to videotape the ventricle.

Calculation of stroke volume. In preliminary studies, the ventricle was videotaped at two angles perpendicular to each other to assess its three-dimensional shape change during different phases of cardiac cycles. Examination of the trace of ventricle outlines from two viewing angles indicated that the ventricle during all phases of the cardiac cycle closely approximated a prolate spheroid. The shape and volume of such spheroids can be derived from length-width dimensions when the spheroid is viewed at a right angle to its long axis. Consequently, all subsequent measurements were based on a single viewing angle, which was perpendicular to the ventricle's long axis.

Ventricular volume (V) was calculated using the formula for a prolate spheroid

$$V = 4/3 \cdot \pi \cdot a \cdot b^2$$

where a and b are the long and short radii, respectively (one-half of the measured long and short axes) of the ventricle. The long and short axes of the ventricle were measured as depicted in Fig. 1. The actual outline of the ventricle was drawn by eye, rather than by edge-defining analytic programs, which were found to be unreliable when applied to these videotaped images. Inherent in these calculations is the assumption that all volume changes of the heart were due to changes in luminal volume, i.e., that even though changes in wall thickness occurred, there was no change in the total volume of the ventricle walls.

The EDV and ESV of three cardiac cycles separated by 5-min intervals were measured, and mean values were calculated for individual animals.

Calculated Variables

The CO for each individual larva was calculated by multiplying mean heart rate for an animal of that body mass, derived from Ref. 15, by mean stroke volume, calculated from actual heart volume changes as described above. Total vascular resistance was calculated by dividing mean truncus blood pressure (from Ref. 15) by cardiac output. An index for cardiac work was obtained by multiplying mean truncus pressure by stroke volume (9). Mean truncus blood pressure, stroke volume, and cardiac output for calculations of vascular resistance and cardiac work were derived from the respective regression lines of this and another study (15). Whereas stroke volume and cardiac output were measured in embryos as small as ~3 mg in the present study, blood pressures were measured in embryos beginning at ~17 mg. Thus values for vascular resistance and cardiac work in 3- to 17-mg larvae are based on interpolations.

Statistical Analysis

All variables are expressed as a function of body mass (on arithmetic or logarithmic scales). A linear regression line by least-squares mean method was calculated for each variable.

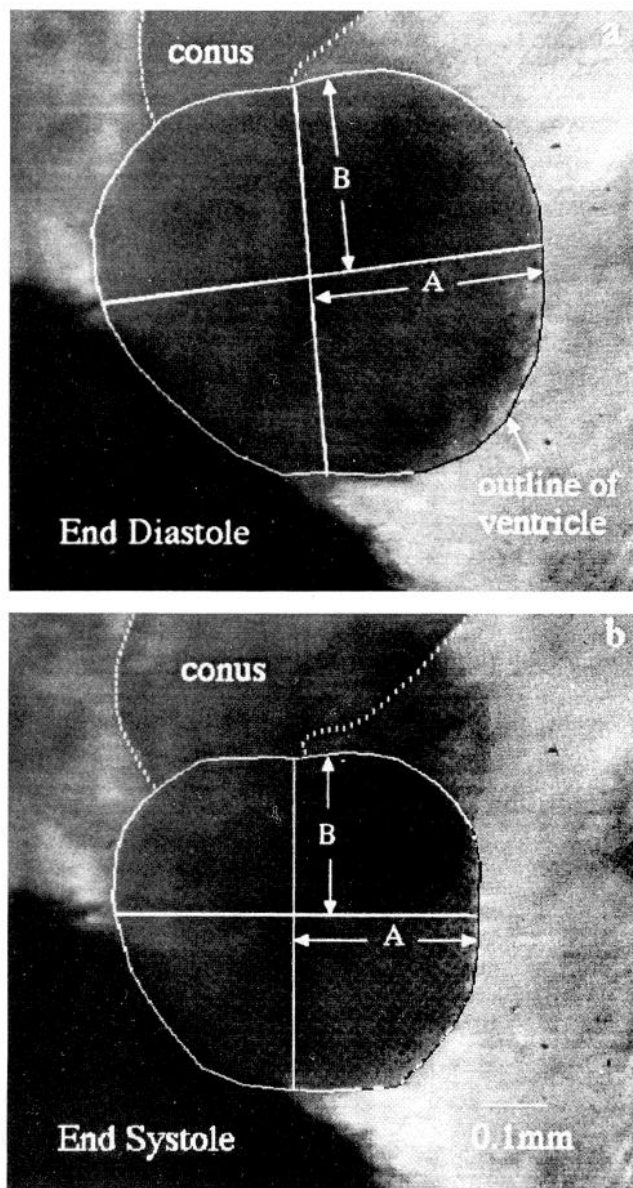


Fig. 1. Video images of ventricle at end diastole (a) and end systole (b) in a 23-mg *Xenopus laevis* at stage 48. Variables measured for calculating ventricular volume are long axis ($2 \times A$), short axis ($2 \times B$), and area enclosed by epicardial outlines. Dashed lines, outlines of conus arteriosus. Both images are on the same scale as shown in b.

Analysis of covariance was made to distinguish the difference between the two regressions. All statistics were performed using a computer program (BIOSTAT I, Sigma Soft, Placentia, CA).

RESULTS

EDV and ESV

EDV of the ventricle increased significantly from $3.7 \times 10^{-3} \mu\text{l}$ at 3 mg to $11.1 \mu\text{l}$ at 1 g (Fig. 2). ESV increased from $4.2 \times 10^{-3} \mu\text{l}$ at 3 mg to $3.5 \mu\text{l}$ at 1 g.

Stroke Volume and Cardiac Output

Stroke volume increased from $2.4 \times 10^{-3} \mu\text{l}$ at 3 mg to $7.6 \mu\text{l}$ at 1 g (Fig. 3). Mass-specific stroke volume also

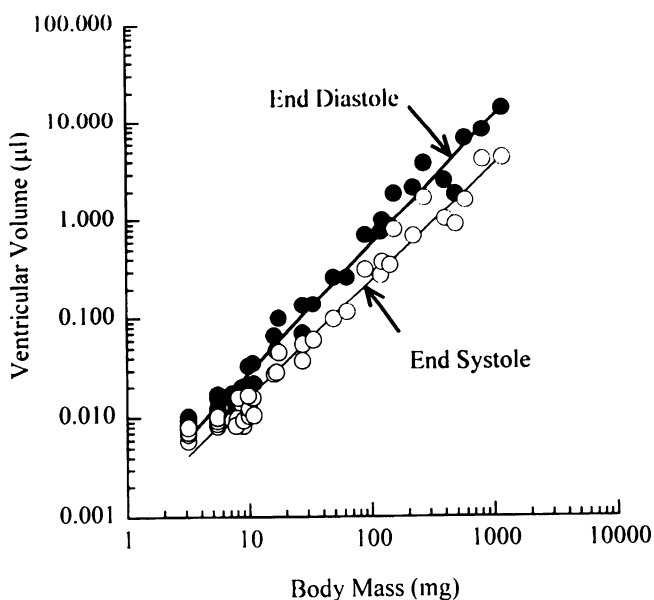


Fig. 2. Ventricular volumes in developing *X. laevis* calculated with prolate spheroid formula at end diastole (●) and end systole (○). Equations of regression lines are given in Table 1.

increased with increasing body mass, i.e., from $7.6 \times 10^{-4} \mu\text{l}/\text{mg}$ at 3 mg to $7.6 \times 10^{-3} \mu\text{l}/\text{mg}$ at 1 g (Fig. 3B).

Cardiac output increased from 0.25 $\mu\text{l}/\text{min}$ at 3 mg to 623 $\mu\text{l}/\text{min}$ at 1 g (Fig. 4A). Mass-specific cardiac output

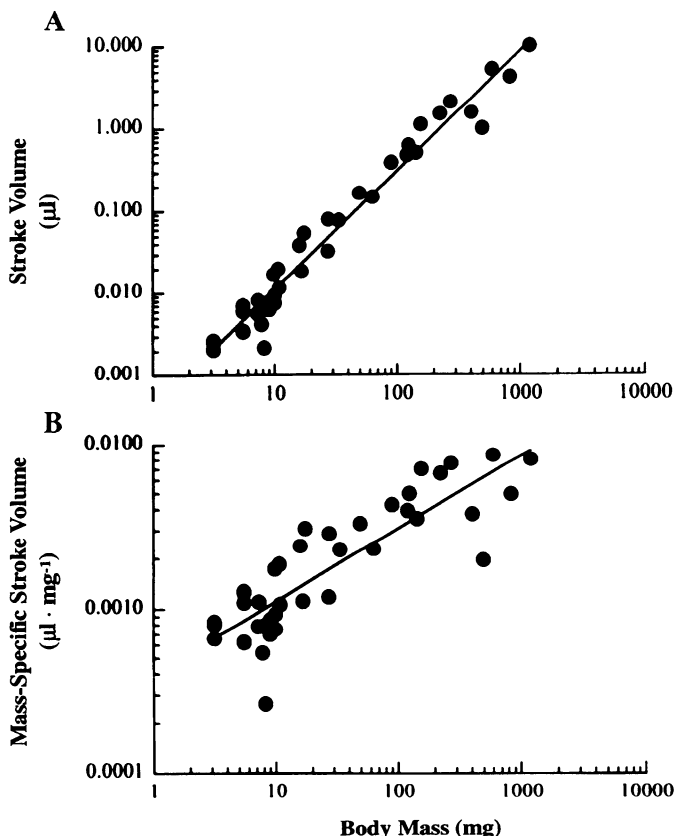


Fig. 3. Stroke volume (A) and mass-specific stroke volume (B), calculated with prolate spheroid formula, in developing *X. laevis*. Values for regression lines are given in Table 1.

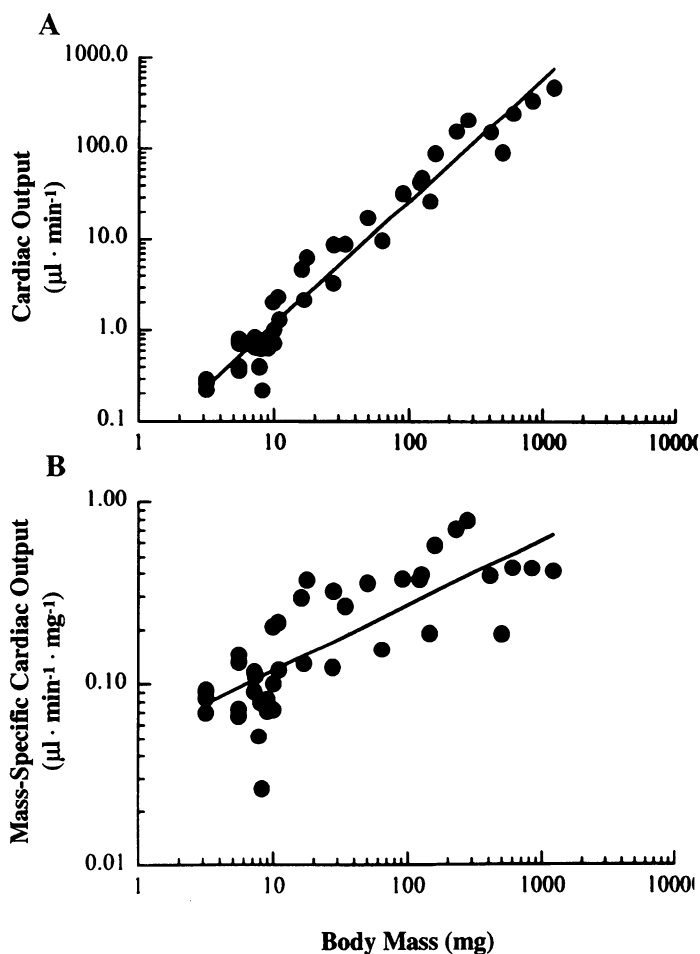


Fig. 4. Cardiac output (A) and mass-specific cardiac output (B) in developing *X. laevis*. Values for regression values are given in Table 1.

also increased from 7.84×10^{-2} to $0.62 \mu\text{l} \cdot \text{min}^{-1} \cdot \text{mg}^{-1}$ between 3 mg and 1 g body mass (Fig. 4B).

Peripheral Vascular Resistance

Peripheral vascular resistance, calculated from the regressions of cardiac output (Table 1) and arterial blood pressure (15), showed an asymptotic decrease with increasing body mass (Fig. 4). Peripheral resistance decreased precipitously from 701 peripheral resistance units (PRU, $\text{mmHg} \cdot \text{s} \cdot \text{mm}^{-3}$) at 3 mg body mass to 79 PRU at 20 mg and gradually declined toward 0.9 PRU at 1,000 mg. On a log-log plot, resistance decreased linearly (Fig. 5).

Cardiac Work

Calculated cardiac work increased from 0.06 $\text{dyn} \cdot \text{mm}$ at 3 mg to 1.27 $\text{dyn} \cdot \text{mm}$ at 20 mg and then climbed sharply to 717 $\text{dyn} \cdot \text{mm}$ at 1,000 mg. Cardiac work increased linearly when expressed on logarithmic scales (Fig. 6).

DISCUSSION

Critique of Methods

The measurement of stroke volume in vertebrate embryos with use of magnified visual images was first

Table 1. Relationships between cardiovascular variables and body mass in *Xenopus laevis*

<i>y</i>	<i>n</i>	log <i>a</i>	<i>b</i>	<i>r</i> ²	<i>P</i>
EDV	43	-2.843	1.296 ± 0.043	0.978	< 0.01
ESV	43	-2.956	1.168 ± 0.039	0.974	< 0.01
SV	43	-3.319	1.399 ± 0.056	0.960	< 0.01
SV*	43	-3.319	0.399 ± 0.045	0.664	< 0.01
CO	43	-1.285	1.360 ± 0.056	0.957	< 0.01
CO*	45	-1.285	0.360 ± 0.046	0.610	< 0.01
<i>R</i>		3.310	-1.115		
<i>W</i>		-1.851	1.618		

Values for *b* are means ± SE. Relationships are expressed as $\log y = \log a + b \cdot \log M$, where *M* is body mass (in mg). EDV and ESV, end-diastolic and end-systolic volumes (in μl), respectively; SV, stroke volume (in μl); CO, cardiac output (in $\mu\text{l}/\text{min}$); *R*, peripheral vascular resistance (in peripheral resistance units, $\text{mmHg} \cdot \text{s} \cdot \mu\text{l}^{-1}$); *W*, cardiac work (in $\text{dyn} \cdot \text{mm}$). Measurements are based on prolate spheroid formula (see text for details). *Mass-specific values. *n*, *r*, and *r*², sample size, coefficient of correlation, and coefficient of determination for correlation, respectively. All regressions and correlations are significant at *P* < 0.01.

used for the heart of the chick (12). The advent of computerized analysis of videotaped images has greatly facilitated analysis of different phases of single cardiac cycles. Yet several complicating factors may affect the accuracy of ventricular volume measurements by video recording techniques.

Measurements of EDV and ESV based on the epicardial outline include the volume of the ventricle walls. Although wall thickness surely changes during the cardiac cycle, the wall itself is largely noncompressible, and its volume should not change appreciably during the cardiac cycle. Consequently, stroke volume measured as the difference between estimated EDV and ESV should represent the true change in ventricular blood volume during each cardiac cycle.

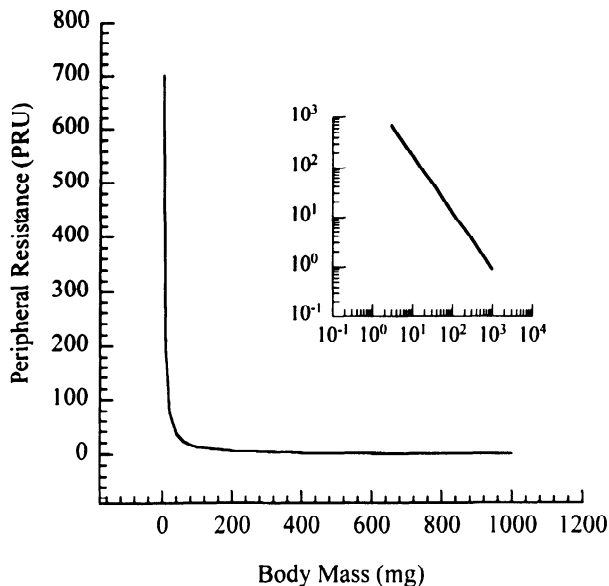


Fig. 5. Peripheral vascular resistance in developing *X. laevis*. PRU, peripheral resistance unit ($\text{mmHg} \cdot \text{s} \cdot \text{mm}^{-3}$). Curve is generated from data points calculated from regressions of mean arterial pressure (Ref. 15) and cardiac output in Table 1. Inset: data plotted on log-log axes. Equation of line is given in Table 1.

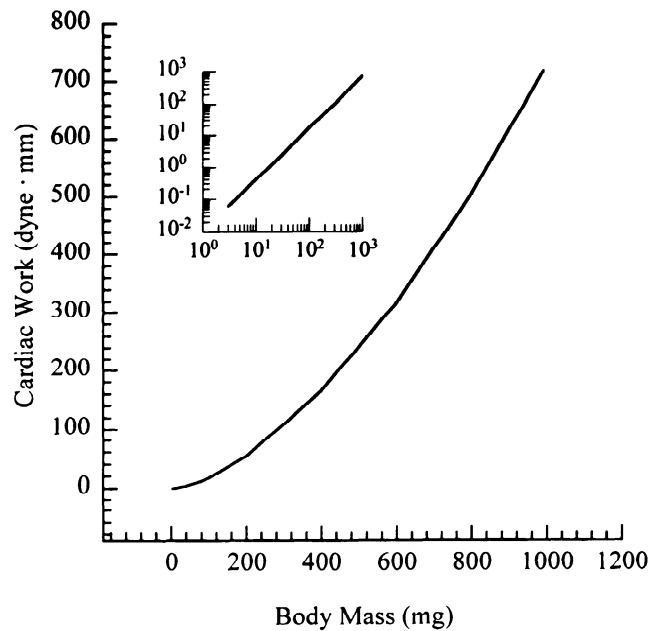


Fig. 6. Cardiac work in developing *X. laevis*. Curve is generated from data points calculated from regressions of mean arterial pressure (Ref. 15) and cardiac output in Table 1. Inset: data plotted on log-log axes. Equation of line is given in Table 1.

The frame rate of image acquisition can also affect selection of the true end-diastolic and end-systolic video images. The video system used in this study acquired and displayed consecutive video fields at a rate of 30 Hz, which allows 15 frames/cardiac cycle at heart rate of 120 beats/min. This sampling rate should provide enough temporal resolution for the current study, inasmuch as heart rates of *Xenopus* larvae usually do not exceed 120 beats/min.

Stroke Volume

Mass-specific stroke volumes in older larval and juvenile *Xenopus* measured in this study exceed those of adult anurans and neotenic amphibians reported in the literature (Table 2). Using electromagnetic flowmeters, Shelton (27) measured blood flows of 0.044 and 0.013 ml/s in the systemic and pulmonary arches, respectively, from one side of the body in a 104-g adult *Xenopus*. Cardiac output calculated from these data is 6.84 ml/min (not including blood to the carotid arches, which leads to an underestimate of flow). At a heart rate of 40 beats/min, stroke volume will be 0.17 ml in a 104-g *Xenopus*. Hoyt et al. (17) calculated a stroke volume of 0.044 ml, which is 25% of that calculated from data reported by Shelton (27), for a 90- to 150-g adult *Xenopus*. Nevertheless, calculated mass-specific stroke volume of the adult *Xenopus* based on data reported by Shelton, 1.63×10^{-3} ml/g, is equivalent to a 35-mg larva, as determined in the present study. Shelton and Jones (28), using a fluid displacement method, showed stroke volume of 0.035 ml in a 21-g *Rana pipiens*. However, in a later study by the same authors (29) using cine photography (similar to the video recording method of the current study), a stroke volume of 0.15 ml was measured in a 20- to 30-g *R. pipiens*. From the latter

Table 2. Literature values for heart rate, stroke volume, and cardiac output in amphibians

	Stage of Development	Sample Size	Body Mass, g	Heart Rate, beats/min	Stroke Volume, ml·g ⁻¹ ·10 ⁻⁴	Cardiac Output, ml·min ⁻¹ ·g ⁻¹	Ref.
<i>Amphiuma tridactylum</i>	Adult	1	750	—	9.3	0.030	19
<i>Ambystoma tigrinum</i>	Neotenus	5	105	62	17.1	0.106	17
<i>Rana catesbeiana</i>	Adult	80	269	30	25.3	0.076	4, 32
<i>Rana pipiens</i>	Adult	1	20–30	47	50.0–75.0	0.237–0.355	29
	Adult	1	21	69	16.7	0.114	28
<i>Rana temporaria</i>	Adult	1	35	60	10.3	0.063	29
<i>Xenopus laevis</i>	Adult	1	104	40	16.3	0.066	28
	Larva (NF stage 40)		0.002	116	6.7	0.078	Present study
	Larva (NF stage 51)		0.1	89	31.8	0.284	Present study

NF, Nieuwkoop-Faber staging system for larval development.

data (29), we calculate a mass-specific stroke volume of 5×10^{-3} – 7.5×10^{-3} ml/g in adult *R. pipiens*. In the neotenic *Ambystoma tigrinum*, stroke volume is 0.18 ml at a mean body mass of 105 g (17), again showing a much smaller mass-specific value than a 100-mg *Xenopus* larva.

Besides *Xenopus*, chick embryos are the only vertebrate species in which stroke volume early in development has been determined. Because our other study (15) has shown that patterns of blood pressure development are very similar in these two vertebrates, we have also compared developmental changes in mass-specific stroke volume during development in these two species. The pattern of change in mass-specific stroke volume during development of larval *Xenopus* is qualitatively quite different from that in chick embryos (Fig. 7). In larval *Xenopus*, absolute stroke volume increases more rapidly than body mass; i.e., the slope of the regression line is > 1 (Table 1). However, in chick embryos, the increase in absolute stroke volume is slower than the increase in body mass; i.e., the slope of the regression line is < 1 (Fig. 7A; data from Ref. 18).

Growth of the heart probably is the most important factor influencing the increase in mass-specific stroke volume in developing *Xenopus* larvae. A close relationship was found between heart mass and stroke volume in mammals (26). Furthermore a parallel relationship between the growth of heart mass and the increase in stroke volume was also found in the chick embryo. Ventricular mass in the chick embryo increased with increasing embryonic mass to the power of 0.85 (11). Interestingly, the calculated relationship between stroke volume and body mass is 0.80 for the chick embryo (Fig. 7A). If this is the case for larval *X. laevis*, ventricular mass should increase faster than body mass.

Cardiac Output

Total cardiac output increased more rapidly than body mass over the range 1–1,000 mg ($b = 1.36$). In the youngest developmental stages, a considerable proportion of “body mass” in fact consists of nonperfused lipids stored in the attached yolk sac and elsewhere. As development progresses, more and more of this material is converted to metabolizing tissue requiring perfusion, presumably being reflected in a rate of increase in demand for cardiac output that exceeds the rate of increase in body mass. Mass-specific cardiac output

increased during early development. Data from a range of body mass of adult animals indicates that mass-specific cardiac output decreases slowly as body mass increases, paralleling a decrease in mass-specific oxygen consumption (26). The present data for cardiac output show that allometric relationships derived from large mature animals cannot be applied in a simple fashion to smaller animals passing through intense periods of organogenesis.

Mass-specific cardiac output in all amphibian larvae that have been examined, including *Xenopus*, is larger than that in adult *Xenopus* (Table 2). Mass-specific cardiac output in other adult or neotenic amphibians,

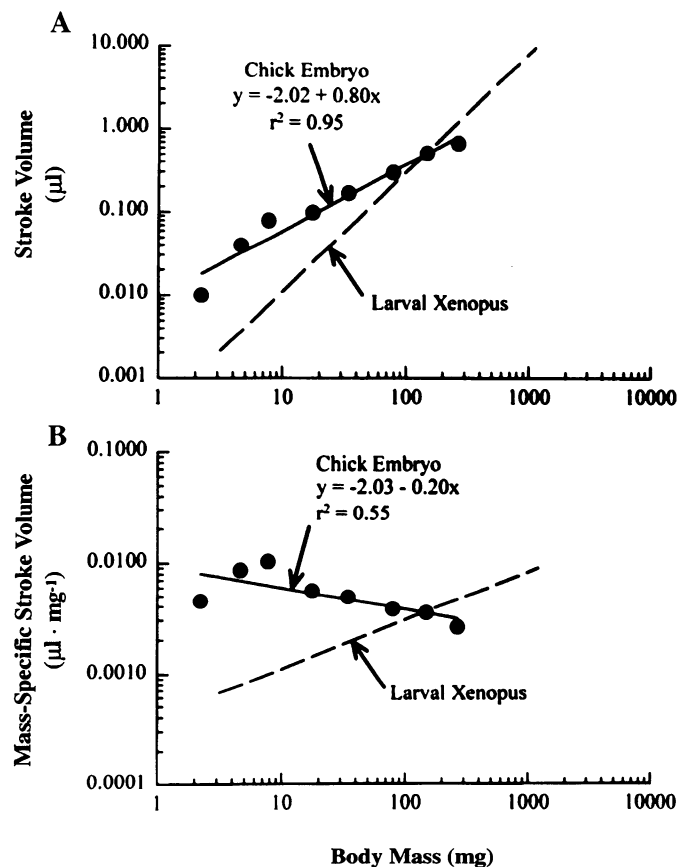


Fig. 7. Stroke volume (A) and mass-specific stroke volume (B) in chick embryos (solid lines) and *Xenopus* larvae (dashed line). Plotted points for chick were calculated using data from Ref. 18. Regression equations and statistics for calculated chick data are indicated.

ranging from $0.03 \text{ ml} \cdot \text{min}^{-1} \cdot \text{g}^{-1}$ in a 750-g *Amphiuma* to $0.24\text{--}0.36 \text{ ml} \cdot \text{min}^{-1} \cdot \text{g}^{-1}$ in a 20- to 30-g *R. pipiens*, is also lower than that in a 120-mg *Xenopus* larva (Table 2). Collectively, these data suggest a decline of mass-specific cardiac output after metamorphosis in amphibians.

The increase of cardiac output during larval development of *X. laevis* is due completely to the increase in stroke volume, because heart rate declines during larval development (15). The increase in stroke volume also accounts for most of the increase of cardiac output during development in the chick embryo. Hu and Clark (18) reported a 120-fold increase in cardiac output in chick embryos from $1.2 \mu\text{l}/\text{min}$ at stage 12 to $144 \mu\text{l}/\text{min}$ at stage 29. However, heart rate increased only twofold over the same period of development.

Cardiac output in larval *X. laevis* is lower than that in chick embryos of similar body mass. The elevated cardiac output in chick embryos may reflect the higher body temperature of chicks. For example, cardiac output in a 4.6-mg chick embryo at stage 14 at 38°C is $4.8 \mu\text{l}/\text{min}$ (18), which is 10 times that of a 4.6-mg *Xenopus* at $21\text{--}24^\circ\text{C}$. Cardiac output after correction for temperature difference is $1.42 \mu\text{l}/\text{min}$ at 38°C , with the assumption of a Q_{10} of 2. The remaining large difference in cardiac output, after a temperature correction, between *Xenopus* and chick embryos may reflect the greater metabolic requirement in avian embryos than in anuran larvae (13). The higher cardiac output in avian embryos may also be correlated with the high capillary density of the enormous extraembryonic circulation of the avian egg. The difference in mass-specific CO between *Xenopus* and the chick decreases as progressively larger embryos are compared. Cardiac output in a 270-mg chick embryo at stage 29 is only 40% greater than that in *Xenopus* of the same body mass, even with no temperature correction.

Peripheral Vascular Resistance

The decrease in vascular resistance during development that we observed in *X. laevis* has also been observed in developing bullfrog larvae (20) and chick embryos (18). Vascular resistance measured by experimental perfusion of the circulation is $2.5\text{--}0.15$ PRU in 4.5- to 8.5-g larval *Rana catesbeiana* (20). These values are higher than those predicted for a *Xenopus* of similar size. However, vascular resistance in adult *Xenopus* calculated from mean arterial pressure (30) and cardiac output (27) is 0.25 PRU. This value is considerably lower than that in larvae, indicating a decrease in vascular resistance after metamorphosis. In chick embryos, vascular resistance decreases from 24.71 PRU at 2.2 mg to 0.63 PRU at 267.5 mg. These values are much lower than those in *Xenopus* larvae of similar body mass.

Changes in vascular resistance during development could result from an increase in cross-sectional area produced by growth of existing vessels as well as addition of new vascular beds in parallel to the existing ones (6). Growth of the vessels also results in an increase in vascular length, which increases vascular resistance. Because vascular resistance is inversely proportional to

the second power of vascular cross-sectional area, the effect of increase in vascular diameter on vascular resistance is more prominent than the length effect during development. Developmental changes in vascular reactivity, which influences in vivo vascular diameter, could also affect vascular resistance during development of *Xenopus*.

Cardiac Work

Cardiac work increases during development of larval *Xenopus*, as it does in chick embryos (18). An increase in the number of myocardial cells as well as an increase in percentage of contractile protein within individual myocardial cells during development may account for the increase in cardiac work (11), although this too requires further study in amphibians.

Summary

Except for heart rate, the general pattern of hemodynamic changes during development of *X. laevis* is similar to that of chick embryos (18). Blood pressure, stroke volume, cardiac output, and cardiac work increase and peripheral vascular resistance decreases with increasing body mass during development in both species. However, heart rate decreases in *Xenopus* larvae, whereas it increases in chick embryos. The pattern of blood pressure development in the skate (23) and most other anuran larvae (3, 24) is also very similar to that of *Xenopus*. Although more studies in piscine, reptilian, and mammalian embryos are needed, strong commonalities in amphibian and avian hemodynamics during development suggest a common pattern for hemodynamic development in vertebrate embryos/larvae. The chick embryo has served as the major model for studies of hemodynamic development in the mammalian embryo. However, because all vertebrate embryos/larvae examined so far seem to display patterns of developmental change quite similar to those of the chick, the choice of an animal model for future studies may be based more on experimental convenience than "phylogenetic appropriateness."

We thank Willy E. Bemis for using his video recorder and image analysis system and E. A. Connor, M. A. Olivo, and J. L. Roberts for comments on earlier versions of the manuscript.

This study, which was part of a Ph.D. dissertation at the University of Massachusetts (Amherst, MA), was supported by National Science Foundation Grants DCB-8916938 and IBN-9307832 to W. W. Burggren and NSC 82-0209-B-006-095-T to P.-C. L. Hou.

Address for reprint requests: P.-C. L. Hou, Dept. of Biology, National Cheng Kung University, Tainan, Taiwan, ROC.

Received 21 April 1994; accepted in final form 12 April 1995.

REFERENCES

1. Benson, D. W., Jr., S. F. Hughes, N. Hu, and E. B. Clark. Effect of heart rate increase on dorsal aortic flow before and after volume loading in the stage 24 chick embryo. *Pediatr. Res.* 26: 438-441, 1989.
2. Burggren, W. W. Central cardiovascular function in amphibians: qualitative influences of phylogeny, ontogeny and seasonality. In: *Mechanisms of Systemic Regulation: Respiration and Circulation*, edited by N. Heisler. Berlin: Springer-Verlag, 1995, vol. 1, chap. 9, p. 1-17.

3. **Burggren, W. W., J. E. Bicudo, M. L. Glass, and A. S. Abe.** Development of blood pressure and cardiac reflexes in the frog *Pseudis paradoxus*. *Am. J. Physiol.* 263 (Regulatory Integrative Comp. Physiol. 32): R602–R608, 1992.
4. **Burggren, W. W., and M. Doyle.** Ontogeny of heart rate regulation in the bullfrog, *Rana catesbeiana*. *Am. J. Physiol.* 251 (Regulatory Integrative Comp. Physiol. 20): R231–R239, 1986.
5. **Burggren, W. W., and J. J. Just.** Developmental changes in amphibian physiological systems. In: *Environmental Physiology of the Amphibians*, edited by M. E. Feder and W. W. Burggren. Chicago, IL: University of Chicago Press, 1992, p. 467–530.
6. **Burggren, W. W., and A. W. Pinder.** Ontogeny of cardiovascular and respiratory physiology in lower vertebrates. *Annu. Rev. Physiol.* 53: 107–135, 1991.
7. **Clark, E. B.** Functional aspects of cardiac development. In: *Growth of the Heart in Health and Disease*, edited by R. Zak. New York: Raven, 1984, p. 81–103.
8. **Clark, E. B.** Functional characteristics of the embryonic circulation. In: *The Development of the Vascular System*, edited by R. N. Feinberg, G. K. Sherer, and R. Auerbach. Basel: Karger, 1991, p. 125–135.
9. **Clark, E. B., and N. Hu.** Developmental hemodynamic changes in the chick embryo stages 18 to 27. *Circ. Res.* 51: 810–815, 1982.
10. **Clark, E. B., N. Hu, and J. B. Dooley.** The effect of isoproterenol on cardiovascular function in the stage 24 chick embryo. *Teratology* 31: 41–47, 1985.
11. **Clark, E. B., N. Hu, J. L. Dummett, G. K. Vandekieft, C. Olson, and R. J. Tomanek.** Ventricular function and morphology in the chick embryo stage 18 to 29. *Am. J. Physiol.* 250 (Heart Circ. Physiol. 19): H407–H413, 1986.
12. **Faber, J. J., T. J. Green, and K. L. Thornburg.** Embryonic stroke volume and cardiac output in the chick. *Dev. Biol.* 41: 14–21, 1974.
13. **Gatten, R. E., Jr., K. Miller, and R. J. Full.** Energetics at rest and during locomotion. In: *Environmental Physiology of the Amphibians*, edited by M. E. Feder and W. W. Burggren. Chicago, IL: The University of Chicago Press, 1992, p. 314–377.
14. **Girard, H.** Arterial pressure in the chick embryo. *Am. J. Physiol.* 224: 454–460, 1973.
15. **Hou, P.-C. L., and W. W. Burggren.** Blood pressures and heart rate during larval development in the anuran amphibian *Xenopus laevis*. *Am. J. Physiol.* 269 (Regulatory Integrative Comp. Physiol. 38): R1120–R1125, 1995.
16. **Howe, R. S., W. W. Burggren, and S. J. Warburton.** Fixed patterns of bradycardia during late embryonic development in domestic fowl with *C* locus pleiotropic mutations. *Am. J. Physiol.* 268 (Heart Circ. Physiol. 37): H56–H60, 1994.
17. **Hoyt, R. W., M. Eldridge, and S. C. Wood.** Noninvasive pulsed Doppler determination of cardiac output in an unanesthetized neotenic salamander, *Ambystoma tigrinum*. *J. Exp. Zool.* 230: 491–493, 1984.
18. **Hu, N., and E. B. Clark.** Hemodynamics of the stage 12 to stage 29 chick embryo. *Circ. Res.* 65: 1665–1670, 1989.
19. **Johansen, K.** Cardiovascular dynamics in the amphibian *Amblystoma tridactylum* Cuvier. *Acta Physiol. Scand.* 60, Suppl. 217: 1–82, 1963.
20. **Kimmel, P. B.** *The Ontogeny of Cardiovascular Regulatory Mechanisms in the Bullfrog (Rana catesbeiana)* (Ph.D. dissertation). Amherst, MA: University of Massachusetts, 1990.
21. **Nieuwkoop, P. D., and J. Faber.** *Normal Table of Xenopus laevis (Daudin)*. Amsterdam: North-Holland, 1967.
22. **Orlando, K., and A. Pinder.** Larval cardiorespiratory ontogeny and allometry in *Xenopus laevis*. *Physiol. Zool.* 68: 65–73, 1995.
23. **Pelster, B., and W. E. Bemis.** Ontogeny of heart function in the little skate, *Raja erinacea*. *J. Exp. Biol.* 156: 387–398, 1991.
24. **Pelster, B., and W. W. Burggren.** Central arterial hemodynamics in larval bullfrog (*Rana catesbeiana*): developmental and seasonal influences. *Am. J. Physiol.* 260 (Regulatory Integrative Comp. Physiol. 29): R240–R246, 1991.
25. **Pelster, B., W. Burggren, S. Petrou, and I. Wahlqvist.** Developmental changes in the acetylcholine influence on heart muscle of *Rana catesbeiana*: in situ and in vitro effects. *J. Exp. Zool.* 267: 1–8, 1993.
26. **Schmidt-Nielsen, K.** *Scaling: Why Is Animal Size So Important?* New York: Cambridge University Press, 1984.
27. **Shelton, G.** The effect of lung ventilation on blood flow to the lungs and body of the amphibian, *Xenopus laevis*. *Respir. Physiol.* 9: 183–196, 1970.
28. **Shelton, G., and D. R. Jones.** Central blood pressure and heart output in surfaced and submerged frogs. *J. Exp. Biol.* 42: 339–357, 1965.
29. **Shelton, G., and D. R. Jones.** Pressure and volume relationships in the ventricle, conus and arterial arches of the frog heart. *J. Exp. Biol.* 43: 479–488, 1965.
30. **Shelton, G., and D. R. Jones.** A comparative study of central blood pressures in five amphibians. *J. Exp. Biol.* 49: 631–643, 1968.
31. **Tazawa, H., T. Hiraguchi, O. Kuroda, S. Tullett, and D. Deeming.** Embryonic heart rate during development of domesticated birds. *Physiol. Zool.* 64: 1002–1022, 1991.
32. **Tazawa, H., M. Mochizuki, and J. Piiper.** Respiratory gas transport by incompletely separated double circulation in the bullfrog, *Rana catesbeiana*. *Respir. Physiol.* 36: 77–95, 1979.